International Journal of Environmental Science and Technology (2020) 17:4759–4774
https://doi.org/10.1007/s13762-020-02761-6

ORIGINAL PAPER

Optimizing binary biosorption of cobalt and nickel ions on brown algae using a central composite design

M. Khajavian[1] · A. Hallajsani[2] · P. Ghelichi[3]

Received: 28 November 2019 / Revised: 8 April 2020 / Accepted: 4 May 2020 / Published online: 14 May 2020

Abstract

One of the most valuable approaches to eliminate heavy metal ions from aqueous solutions is biosorption. Cobalt and nickel can be removed from aqueous solutions simultaneously using sodium chloride-treated *Cystoseria indica*, which is a kind of brown algae. Three parameters, including pH, initial concentration of heavy metals, and adsorbent mass, were designated to run batch adsorption experiments. The central composite design was employed to show the simultaneous change of all factors according to a pre-specified experimental matrix that creates a response model in which the interactions between the calculated responses and each variable as well as interaction influences, are revealed. R^2 values for the computed model were 0.96 and 0.95 for the response surface 1 (cobalt) and 2 (nickel), respectively. Central composite design calculated the optimum adsorption process as pH, 5.9; biomass dosage, 0.06 g; initial nickel concentration, 91.94 mg/l; and initial concentration of cobalt 89.36 mg/l. The kinetic and isotherm models were engaged to evaluate the equilibrium data at the optimum condition. The biosorption of both heavy metal ions obeyed the intra-particle diffusion kinetic model best, with the equilibrium adsorption time at 80 min. The extended Freundlich isotherm model is better fitted for the equilibrium biosorption data of nickel and cobalt ions. The maximum biosorption of nickel and cobalt ions simultaneously at optimized condition was 69.99 and 75.21 mg/g, respectively.

Keywords Algae · Heavy metal biosorption · Optimization

Introduction

Releasing heavy metals into the environment has turned into universal problematic matters. Many industries are a participant in unleashing toxic metals into the natural environment, which can result in the entering of heavy metals into the human and animal food chain. The accumulation of toxic heavy metals can endanger human health (Salehi and Madaeni 2014). Oil, gas, textile, battery industries evacuate heavy-metal contaminants like nickel (Ni) and cobalt (Co) (Luo et al. 2018; Xu et al. 2013). Heavy metal ions tend to accumulate in the human body and the natural environment (Park et al. 2015). Biosorption (based on the biological materials to remove the heavy metals) (Ozdemir et al. 2020), adsorption (mass conversion method) (Ojedokun and Bello 2016), reverse osmosis (based on the principle of size exclusion and charge exclusion) (Hosseini et al. 2016), chemical precipitation (adding chemicals to form metal precipitation) (Nas et al. 2019), ion exchange (substituting the ions with another) (Bila et al. 2013), and membrane filtration (pressure-driven separation technique) (Daraei et al. 2013) can be used to remove heavy metals from aqueous solutions. The biosorption process is regarded as one of the most effective ways of heavy metals removal for its outstanding features, including low-priced, eco-friendly, renewability and large biosorption capacity. Biosorption includes the passive binding to metabolic inactive materials stemmed from industrial or agricultural by-products, forestry, marine or terrestrial biological materials and microbe biomass. Macroalgae biomass is broadly available and comprises various active sites,

Editorial responsibility: Fatih ŞEN.

✉ M. Khajavian
mohamadkhajavian@gmail.com

[1] Chemical Engineering Department, Arak University, Arak, Iran

[2] Chemical Engineering Department, Tehran University, Tehran, Iran

[3] Chemical Engineering Department, Kashan University, Kashan, Iran

including hydroxyl, carboxyl and amine, in its cell buildings that are reachable for heavy metal ions (Liang et al. 2019).

Many studies have reported that biosorbents comprising bacteria, fungi, algae have the exceptional capability to adsorb heavy metal ions (Kim et al. 2017; Taghi Ganji et al. 2005; Kajavian et al. 2019; Li et al. 2018).

Brown algae biomass has attracted much attention as a biosorbent because of non-toxic nature, renewability, abundance in the natural environment, and catalytic features in the adsorption process (Esmaeili and Aghababai 2015). The biosorption aptitudes of the brown algae, as macroalgae, can be ascribed to the presence of carboxylic acid, sulfonic acid, and amide groups (Akbari et al. 2015; Montazer-Rahmatia et al. 2011).

The northern coast of the Gulf of Oman is recognized as the most abundant source of macroalgae. *Cystoseria indica* (*C. indica*) is a subclass of brown algae that can be found plentifully in the Gulf of Oman (Sinaeia et al. 2018; Negm et al. 2018). Growing in huge dimensions and including alginic acid make the usage of *C. indica* reasonable in removing heavy metals from aqueous solutions (Rasool et al. 2015; John Babu et al. 2019). Oil–gas wastes and heavy metals discharging into the marine environment can impact the ecosystem of aquatic beings in the Gulf of Oman harmfully (Ferraz et al. 2015; Sinaei et al. 2018). Therefore, *C. indica* is an effective biosorbent to eliminate the contamination from the Gulf of Oman.

Current study focused on the optimization of simultaneous adsorption of two heavy metal ions (cobalt and nickel) to maximize the removal capacity of macroalgae, considering operational condition, and using central composite design. Not only, central composite design minimizes the number of experimental runs, but also displays the interaction between operational variables, and interaction among operational variables and removal efficiency. Sodium chloride was used to treat the surface of brown algae (*Cystoseria indica*), which is derived from the Oman Sea, to increase the steadiness and the heavy metal adsorption capacity of the brown algae. The optimum amount of pH, adsorbent mass, initial concentration of Co, and initial concentration of Ni was attained using the central composite design algorithm of Design-Expert software. ATR-FTIR spectrometer and scanning electron microscopy (SEM) were utilized to characterize the surface of *C. indica*. Moreover, isotherm and kinetic models were assessed suing biosorption equilibrium data at optimum conditions.

Materials and methods

Materials

The stock solution of Co (Co(II)) and Ni (Ni(II)) was prepared by dissolving Co nitrate (Co $(NO_3)_2.4H_2O$) and Ni nitrate (Ni $(NO_3)_2{\cdot}6H_2O$) in distilled water. The changed operational concentration of Co(II) and Ni(II) was arranged by dilution of Co(II) and Ni(II) stock solution with deionized water. The solution pH was changed using HCl (0.1 N) and NaOH (0.1 N). All of the chemicals in this study were acquired from Sigma-Aldrich.

Cystoseria indica preparation

Cystoseria indica (*C. indica*) collected from the Oman Sea were initially cleaned with deionized water to eliminate surface from salts and dirt. Sunlight was employed to desiccate the clean algal samples. Dried *C. indica* were sieved to the size of 0.5–1.0 mm, after drying with the sun for twenty-four hours. Afterward, the sieved *C. indica* were desiccated in an oven at 70 °C for twenty-four hours, after washing with deionized water. According to the previous studies, sodium chloride (NaCl) was used to treat the surface of *C. indica* macroalgae to raise its ability to adsorb heavy metals (Pinnola et al. 2019; Sari and Tuzen 2008).

Batch biosorption of Ni and Co from aqueous solution

According to the pretests and previous studies, pH (2–6), initial metal ion concentrations (30–150 mg/L), adsorbent mass (0.06–0.1 g), and contact times (180 min) were chosen to conduct the biosorption experiments at 25 °C. The algae were added to the containers, including 100 ml of Ni and Co solution, and stirred at 175 rpm for 5 h. After filtering algae, atomic absorption spectroscopy (PinAcle 500, PerkinElmer, USA) was applied to ascertain the residual metal ions concentrations in solutions at the end of adsorption experiments. Equation (1) (equation) calculated the concentrations of the metals adsorbed by *C. indica* (mg/L):

$$q = \frac{V\left(C_i - C_f\right)}{m} \tag{1}$$

C_i and C_f (mg/L) are defined as the initial and, finally, heavy metal concentrations in the solution, respectively. V and m are described as the solution volume (L) and the mass of biosorbent (g), respectively. Input and output streams are stopped during the batch adsorption process, unlike the continuous process.

Experimental design

Adsorption process variables, including the initial concentration of Co, the initial concentration of Ni, adsorbent dose and pH, were optimized to maximize the adsorption capacity of *C. indica* for simultaneous adsorption of Co and Ni using the central composite methodology of Design-Expert

Table 1 Designated levels for variables of central composite design

Factors	Unites	− 1	0	+ 1
Adsorbent mass	g	0.06	0.08	0.1
Initial concentration of adsorbate (Co)	mg/L	30	90	150
Initial concentration of adsorbate (Ni)	mg/L	30	90	150
pH	–	2	4	6

Software (version 11.0.0). Limitations selected for each variable are existing in Table 1. According to the previous studies and the pretests, the level of variables was determined, as shown in Table 1.

The finest circumstances can be determined by optimizing variables to maximize the removal percentage (% removal) of Co and Ni simultaneously using *C. indica* algae. The overall explanation of the response surface is given in Eq. (2) (Khosravi et al. 2017):

$$y = \beta_0 + \sum_{i=1}^{k} \beta_i x_i + \sum_{i=1}^{k} \beta_{ii} X_i^2 + \sum \sum_{i<j} \beta_{ij} x_i x_j + \varepsilon \quad (2)$$

In Eq. (2), y is correlated to the dependent variable, k is the number of inputs (independent) variables, β_0 is a constant, and β_{ii}, β_i, and β_{ij} are linear, quadratic, and interaction regression coefficients, respectively. X_i and X_j are independent factors, and ε is the standard error.

Biosorption isotherm study

The multiple-metal system can impede the adsorption process because heavy metals ions compete to gain active sites on the *C. indica* surface (Hadi et al. 2013). Numerous industries release their wastewaters in the form of multi-metal components, which is the main reason for this study to select the binary system (Villar da Gama et al. 2018). In this study, Langmuir and Freundlich isotherms were evaluated by the equilibrium data at a constant temperature (Sahan 2019; Gupta and Balomajumder 2015).

Langmuir isotherm study

Uniform and monolayer adsorption are the principles of the Langmuir isotherm. The extended Langmuir isotherm can be expressed by Eqs. (2) and (3):

$$q_{e1} = q_{m,1}\left(\frac{K_{L1}C_{e1}}{1 + K_{L1}C_{e1} + K_{L2}C_{e2}}\right) \quad (3)$$

$$q_{e2} = q_{m2}\left(\frac{K_{L2}C_{e2}}{1 + K_{L1}C_{e1} + K_{L2}C_{e2}}\right) \quad (4)$$

K_{L1}, K_{L2}, q_{m1}, q_{m2} are the Langmuir isotherm constants, and C_{e1} (mg/L) and C_{e2} (mg/L) are the residual concentration of Ni and Co at the end of the adsorption process, respectively. The equilibrium data for Ni and Co biosorption can be presented by q_{e1} (mg/g) and q_{e2} (mg/g), respectively (Putro et al. 2017; Gaikwad and Balomajumder 2017).

Freundlich isotherm study

Heterogeneous systems can be defined by Freundlich isotherm. Equations (4) and (5) show extended Freundlich isotherm:

$$q_{e1} = \frac{K_{F1}C_{e1}^{\frac{1}{n_1}+X_1}}{C_{e1}^{x_1} + y_1 C_{e2}^{z_1}} \quad (5)$$

$$q_{e2} = \frac{K_{F2}C_{e2}^{\frac{1}{n_2}+X_2}}{C_{e2}^{x_2} + y_2 C_{e1}^{z_2}} \quad (6)$$

C_{e1} and C_{e2} are the residual concentrations of Ni and Co at the end of the adsorption process, respectively; the unit of C_{e1} and C_{e2} is mg/L. $qe1$ and $qe2$, respectively, can present the equilibrium adsorption values of Ni and Co; q_{e1} and q_{e2} are equal to mg/g. Suffixes 1 and 2 are utilized to signify Ni and Co, respectively.

x_1, y_1, z_1, x_2, y_2, z_2 are the Freundlich isotherm constants. K_{F1}, K_{F2}, n_1, and n_2 are the Freundlich isotherm constants (Fan Huan et al. 2008). The equilibrium data of the separately adsorbed Ni and Co by the *C. indica* were used to calculate Freundlich isotherm constants and are presented in Table 2. Nonlinear regression using MATLAB software was used to evaluate the model parameters. The favorability between the experimental data and the calculated data was measured by the coefficient of determination (R^2), which is calculated using Eq. (7) (Chen et al. 2008; Yalçın et al. 2012). The closeness of R^2 to 1.00 means a better fitting between the experimental data and the computed data.

Table 2 Langmuir and Freundlich isotherm parameters for the separate adsorption of Ni (II) and Co (II) using *C. indica* at 25 °C (Kajavian et al. 2019; Akbari et al. 2015; Montazer-Rahmatia et al. 2011)

Isotherms	Parameters	Ni	Co
Langmuir	q_m (mg/g)	41.11	77.13
	K_L (L/mg)	0.15	0.31
	R^2	0.99	0.94
Freundlich	K_f (mg/g) (L/mg)	19.20	23.21
	n	2.89	1.35
	R^2	0.99	0.99

$$R^2 = 1 - \frac{\sum_{i=1}^{m}(q_i^{exp} - q_i^{cal})^2}{\sum_{i=1}^{m}(q_{ave}^{exp} - q_i^{cal})^2} \quad (7)$$

2.8. Biosorption Kinetic of Ni and Co ions

The contact time of 300 min was determined as equilibrium time for the adsorption processes of Co and Ni using *C. indica* (Nuhoglu et al. 2002; Mudhoo et al. 2012). Pseudo-first-order, pseudo-second-order, and intra-particle diffusion kinetic models were used to describe biosorption kinetic of Co and Ni ions using *C. indica*.

The pseudo-first-order model

The pseudo-first-order model was used to explain the mechanism of the adsorption process. The pseudo-first-order equation can be described by Eq. (9) (Volesky 2001):

$$\frac{dq}{dt} = K_1(q_e - q_t) \quad (8)$$

where q_t (mg g^{-1}) is Ni(II) and Co(II) uptake amount at time t (min), q_e (mg g^{-1}) is the Ni(II) and Co(II) uptake amount at equilibrium, k_1 is the first-order reaction rate constant (min^{-1}).

The pseudo-second-order model

The pseudo-second-order model was utilized to compute pseudo-second-order model parameters, and can be described using Eq. (9) (Hamedy et al. 2000):

$$\frac{dq_t}{dt} = K_2(q_e - q_t)^2 \quad (9)$$

where q_t (mg g^{-1}) is Ni(II) and Co(II) adsorption amount at time t (min), q_e (mg g^{-1}) is the Ni(II) and Co(II) adsorption amount at equilibrium, and k_2 signifies the second order reaction rate constant (g mg^{-1} min^{-1}).

Intra-particle diffusion model

Intra-particle diffusion model was also employed to disclose the mechanism and influence of the rate-controlling step on the adsorption process for the biosorption of Ni and Co using *C. indica* and its linear form is given in Eq. 10 (Nagm et al. 2018).

$$q_t = K_p t^{\frac{1}{2}} + C \quad (10)$$

Equation 10 shows intra-particle diffusion in which C (mg/g) is adsorption constant, and K_p (mg/g.$min^{0.5}$) is described as the rate of intra-particle diffusion, respectively. q_t (mg g^{-1}) is Ni(II) and Co(II) uptake amount at time t (min).

Results and discussion

Characterization of brown algae

A scanning electron microscope (Hitachi SU-70, Japan) was utilized to characterize SEM micrographs of C. indica. A honeycomb structure, nonuniform pore distribution and high roughness could be observed using the SEM image of *C. indica* (Fig. 1).

The surface of *C. indica* comprises different functional groups, including hydroxyl, phenolic, aldehydic, ketonic, and carboxylic, which are the active sites for the adsorption of Ni and Co (Leng et al. 2015). Attenuated total reflectance-Fourier transform infrared (ATR-FTIR, Platinum, Bruker, Germany) analyses were utilized to study the surface of *C. indica*. Figure 2 shows the ATR-FTIR analysis of *C. indica*. The stretching vibration of O–H can be detected at 3400 1/cm, that can be ascribed to hydroxyl functional clusters (Leng et al. 2015). The peak of 2900 1/cm, 1640 1/cm, and 1100 1/cm showed up because of C–H, aromatic CC and, COC= - - bonds, respectively (Xiao et al. 2018; Liu et al. 2009). The high silica substance and oxygen-containing groups of the *C. indica* can be described at a peak of 1037 1/cm (Xiao et al. 2018; Abdulrazzaq et al. 2014).

Experimental design outcomes

Lessening the number of experimental runs and simultaneous evaluation of the interactions among the operating variables are the main advantages of optimizing according to the experimental design. The simultaneous separation of Co and Ni by *C. indica* was evaluated using batch adsorption experiments. Central composite design algorithm of the design expert software delivered the experimental runs, which were conducted several times to authenticate the validity of results. Experimental runs and surface responses are presented in Table 3. The surface responses were the removal of nickel and cadmium. Statistical significance of

Table 3 Runs and the results of Ni and Co removal percentage

Run	Point Type	A pH	B Adsorbent mass	C Initial concentration of Co	D Initial concentration of Ni	Response Removal of Co (%)	Response Removal of Ni (%)
1	Fact	2	0.06	30	150	40	60
2	Fact	4	0.08	90	90	58	42
3	Fact	4	0.08	90	90	58	42
4	Fact	2	0.1	150	150	62	38
5	Fact	4	0.08	90	30	61.3	38.6
6	Fact	4	0.08	30	90	49.2	50.7
7	Fact	6	0.1	30	150	44	56
8	Fact	2	0.06	30	30	55	45
9	Fact	4	0.06	90	90	59	41
10	Fact	4	0.08	90	90	57	43
11	Fact	6	0.06	30	150	41	59
12	Fact	2	0.06	150	30	62	38
13	Fact	2	0.1	30	30	53	47
14	Fact	6	0.1	150	30	65	34.6
15	Fact	4	0.08	90	90	53	47
16	Fact	6	0.06	150	150	64	36
17	Fact	2	0.1	150	30	62	38
18	Fact	6	0.06	150	30	65	35
19	Fact	2	0.1	30	150	40	60
20	Fact	2	0.06	150	150	61	39
21	Fact	6	0.06	30	30	56	44
22	Fact	4	0.1	90	90	56.7	43.2
23	Fact	4	0.08	90	90	59	41
24	Fact	4	0.08	150	90	64	36
25	Fact	6	0.1	30	30	61	39
26	Fact	6	0.08	90	90	60	40
27	Fact	6	0.1	150	150	64	36
28	Fact	4	0.08	90	90	57	43
29	Fact	4	0.08	90	150	51.5	48.4
30	Fact	2	0.08	90	90	55.2	41

Co removal and the variance of the outcomes have been shown in Table 4. The effectiveness of variables on the model response could be detected from *P* values less than 0.05 than the other variables (Khosravi et al. 2017; Salehi et al. 2019; Askari et al. 2019). As shown in Table 4, A (pH), C (initial concentration of Co) and D (initial concentration of Ni) variable proposed a larger impact on the model response for both Co removal as response surface 1. ANOVA (analysis of variance) results can be seen in Table 4. It is evident from the results depicted in Table 4, R^2 value for the calculated model is 0.96 for the response surface 1, which certifies the favorability of the model for describing the biosorption process behavior.

Statistical significance of Ni removal and the variance of the results have been displayed in a Table 5. As shown in Table 5, A (pH), C (initial concentration of Co) and D (initial concentration of Ni) variable proposed a more significant impact on the model response for Ni removal as

Fig. 1 SEM Image of *C. indica*, 20.0 k.x, 25.0 k.x

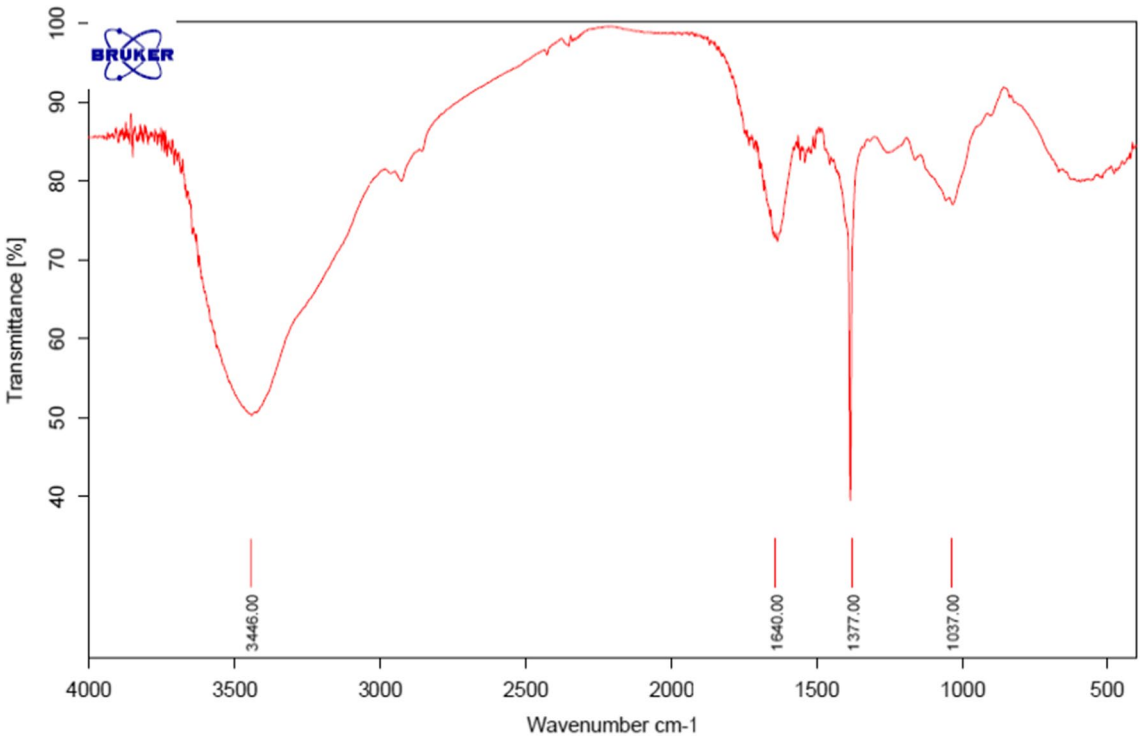

Fig. 2 ATR-FTIR of *C. indica*

Table 4 ANOVA for Co removal model and ANOVA results

Source	Sum of squares	*df*	Mean square	*F* value	*P* value Prob > *F*
Model	1492.88	10	149.29	54.14	0.0001
A pH	49.34	1	49.34	17.89	0.0005
B Adsorbent mass (g)	1.23	1	1.23	0.4450	0.5127
C Initial concentration of Co	936.00	1	936.00	339.43	< 0.0001
D Initial concentration of Ni	294.44	1	294.44	106.77	< 0.0001
AB	5.06	1	5.06	1.84	0.1913
AC	0.5625	1	0.5625	0.2040	0.6566
AD	1.56	1	1.56	0.5666	0.4608
BC	1.56	1	1.56	0.5666	0.4608
BD	0.0625	1	0.0625	0.0227	0.8891
CD	203.06	1	203.06	73.64	< 0.0001
Residual	52.39	19	2.76		
Lack of fit	30.39	14	2.17	0.4934	0.8631
Pure Error	22.00	5	4.40		
ANOVA results	R^2	0.96			

Table 5 ANOVA for Ni removal model and ANOVA results

Source	Sum of squares	*df*	Mean square	*F* value	*P* value Prob > *F*
Model	1487.57	10	148.76	41.92	< 0.0001
A pH	38.72	1	38.72	10.91	0.0037
B Adsorbent mass (g)	1.50	1	1.50	0.4233	0.5231
C Initial concentration of Co	940.33	1	940.33	264.96	< 0.0001
D Initial concentration of Ni	297.68	1	297.68	83.88	< 0.0001
AB	5.52	1	5.52	1.56	0.2274
AC	0.4225	1	0.4225	0.1190	0.7339
AD	1.82	1	1.82	0.5153	0.4823
BC	1.32	1	1.32	0.3726	0.5488
BD	0.0225	1	0.0225	0.0063	0.9374
CD	200.22	1	200.22	56.42	< 0.0001
Residual	67.43	19	3.55		
Lack of fit	45.43	14	3.25	0.7375	0.7014
Pure Error	22.00	5	4.40		
ANOVA results	R^2	0.95			

response surface 2, respectively. ANOVA (analysis of variance) results can be understood in Table 5. It is clear from the outcomes shown in Table 5, R2 value for the computed model is 0.95 for the response surface 2, which confirms the validity of the model for explaining the biosorption behavior of Ni ions using *C. indica*.

The effectiveness of variables was calculated via analysis of variance (ANOVA). Tables 4 and 5 show these variables and the outcome of the fitted model was uttered with accordance to the removal percentage of Co and Ni to define the regression model. Polynomial equations (Eq. 11, 12) were calculated to forecast the response after analyzing the multivariate regression system:

$$\begin{aligned}\text{Removal of Co}\,(\%) =& 56.46 + 1.66 \times A + 0.2611 \times B \\ &+ 7.21 \times C - 4.04 \times D + 0.5625 \\ &\times AB - 0.1875 \times AC - 0.3125 \\ &\times AD - 0.3125 \times BC + 0.0625 \\ &\times BD + 3.56 \times CD\end{aligned} \tag{11}$$

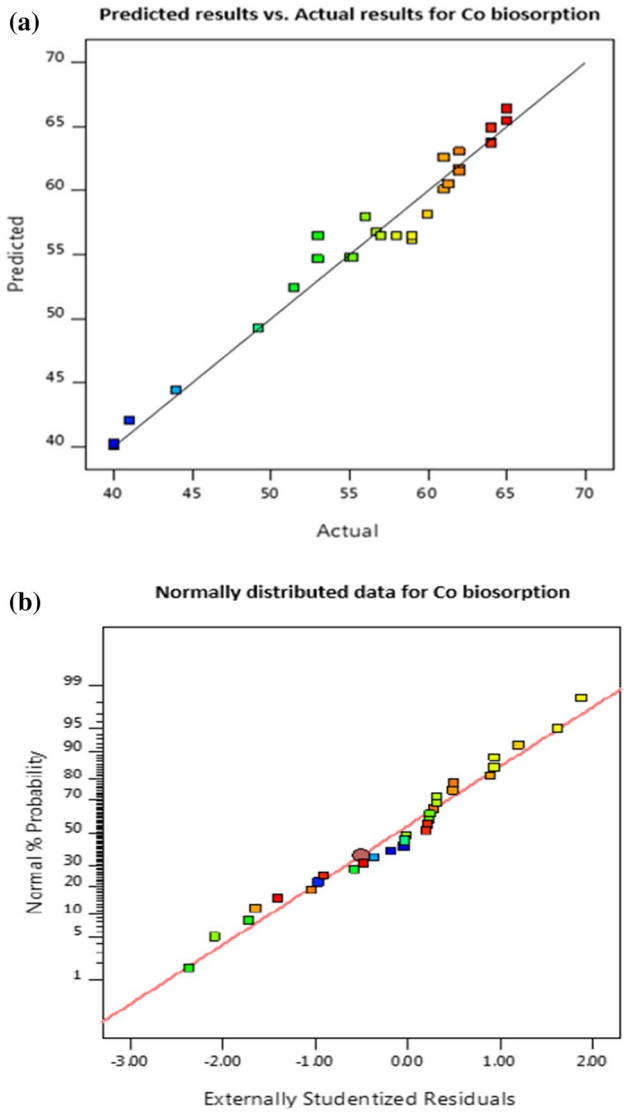

Fig. 3 Comparing the model predicted and the experimental outcomes and, normal distribution of data against calculated data set for Co biosorption

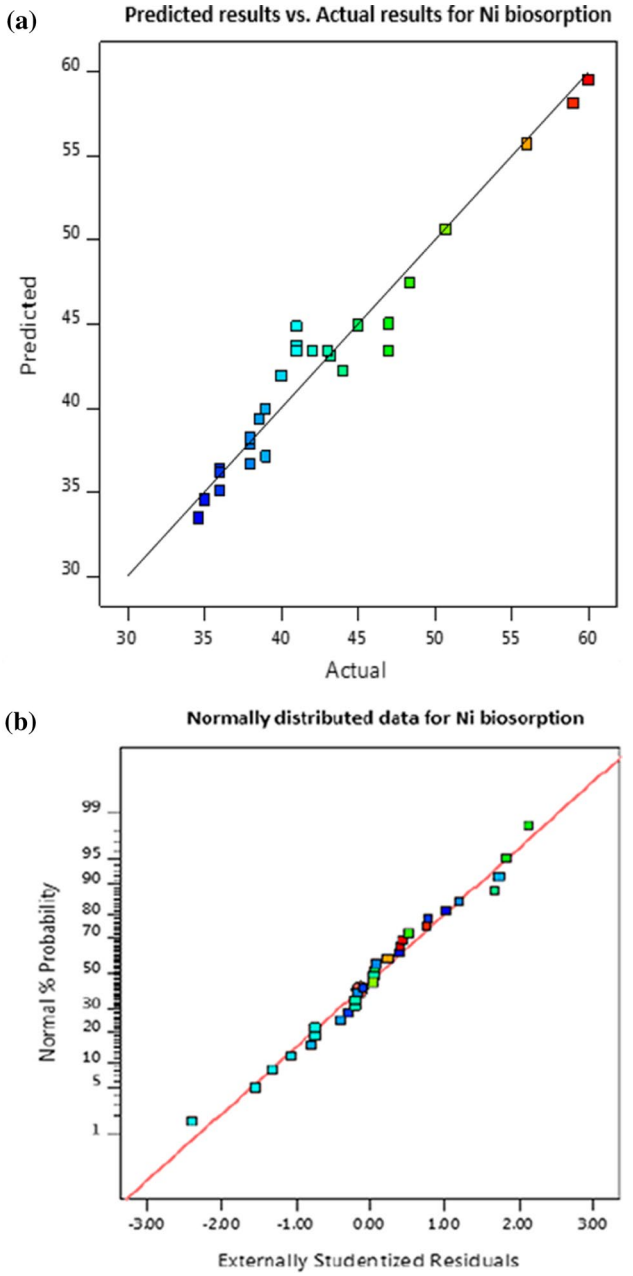

Fig. 4 Comparing the model predicted and the experimental outcomes and, normal distribution of data against calculated data set for Ni biosorption

$$\begin{aligned}\text{Removal of Ni (\%)} =& 43.38 - 1.47 \times A - 0.2889 \times B \\ & - 7.23 \times C + 4.07 \times D + 0.5875 \\ & \times AB + 0.1625 \times AC + 0.3375 \\ & \times AD + 0.2875 \times BC - 0.0375 \\ & \times BD - 3.54 \times CD \end{aligned} \tag{12}$$

In Eq. (11), A, B, C, and D are attributed to pH, adsorbent mass, initial concentration of Co and initial concentration of Ni, respectively. A positive factor signifies that the amount of the response variable changes directly with changing of its vales. Figure 3 contrasts the model predicted and the experimental results surface response 1 (Co removal %) and shows the normal probability chart representing the favorability of points on the linear pattern for surface response 1 (Co removal %).

In Eq. (12), A, B, C, and D are attributed to pH, adsorbent mass, initial concentration of Co and initial concentration of Ni, respectively. Figure 4 compares the model calculated and the experimental outcomes of surface response 2 (Ni removal %) and displays the normal probability chart

indicating the validity of points on the linear pattern for surface response 2 (Ni removal %).

Interactions of variables

Figure 5 illustrates the 3D charts of the two-component interactions of the variables on Co removal through the interaction charts. The interaction among removal, pH and the adsorbent mass to remove Co from solution is revealed in Fig. 5. Upregulating pH can increase the adsorption of Co. Low pH led metal cations and protons to contest for active sites, leading to low adsorption of metal ions. Furthermore, electrostatic repulsion between positively charged surface sites and positive metal cations causes to reduce the adsorption of Co. Increasing pH led to increasing the negativity of active sites that allured more positively charged metal ions for attachment. The biosorbent dosage could not affect the biosorption capacity of *C. indica* to adsorb Co while the more biosorbent dosage means the more active sites that this is due the fact that the process of *C. indica* treatment, using NaCl, did not saturate all of the sites accessible on the NaCl-pretreated *C. indica*.

Figure 6 explains the two-component interactions of the variables on Ni removal using the interaction charts. The interaction among removal, pH, and the adsorbent mass to remove Ni from the solution is exposed in Fig. 6. pH can upregulate the biosorption of Ni. Low pH led metal cations and protons to compete for active sites, resulting in low adsorption of Ni ions. Additionally, electrostatic repulsion between positively charged surface sites and positive metal cations leads to a decrease in the adsorption of Ni. Increasing pH caused to increase the negativity of active sites that trapped more positively charged metal ions for attachment. The more biosorbent dosage means the more active sites, but the biosorbent dosage could not influence the biosorption ability of *C. indica* to remove Ni. This is due the fact that the process of *C. indica* treatment, using NaCl, did not saturate all of the sites accessible on the NaCl-pretreated *C. indica*. The interaction among removal, pH and the initial concentration of Co to remove Co from solution is revealed in Fig. 5. Figure 6 shows the dealings among the removal of Ni, pH and the initial concentration of Co and Ni to eliminate Ni from aqueous solution.

The more initial concentration of Co and Ni, the more removal of Co and Ni. This is because the higher initial heavy metal concentration increases the driving force of the concentration gradient. Higher driving force means more collisions between the heavy metal ions and adsorbents. Also, with an increase in Ni concentration (Fig. 5), it can be seen that the Co removal decreased because of the competitive relationship between Ni and Co to acquire active sites. Figures 5 and 6 reveal that adsorbent mass does not affect the removal of Co when the initial concentration of Ni and Co is increasing.

Published research (Yalçın et al. 2012; De France et al. 2002; Nuhoglu et al. 2002) showed the concentrations ranging from 30 to 150 mg/l could cause the highest capacities of algal adsorption for Ni and Co removal in aqueous solutions when they are in the binary system. Figures 5 and 6 show the interferential effect of metal ions (Co^{2+} and Ni^{2+}) on the removal of each other by *C. indica*.

Comparing Figs. 5 and 6 suggested that *C. indica* tend to adsorb more Co than Ni because Fig. 5 shows that with raising the initial concentration of Co in the presence of Ni, the removal of Co is increasing sharply, which leads to more adsorption of Co in comparison to Ni. But from Fig. 6, it can be seen that increasing the initial concentration of Ni in the presence of Co does not increase the removal of Ni, while the adsorption of Co is rising. Therefore, it can be concluded that Ni is a loser in competition with Co to acquire active sites on the *C. indica* macroalgae. Carboxyl, sulfonic acid and alginate are the main functional groups on the surface of *C. indica* [41]. These functional groups play a key role to adsorb heavy metal ion from aqueous solution. The synergistic effect of Ni and Co ions has been shown in Figs. 5 and 6. Co succeeded in acquiring more active sites on the surface of *C. indica* in the binary system. The higher Co removal can be attributed to the alginic acid component, which exists on the surface of *C. indica* (Mudhoo et al. 2012; Xiong et al. 2013). The characteristics of the adsorbent can be affected meaningfully by the metallic behavior in binary systems (Volesky and Naja 2011; A-Davisa et al. 2003; Senthilkumar et al. 2006).

The optimal conditions were obtained as: pH of 5.9, the adsorbent mass of 0.06 g, initial concentration of Ni 91.94 mg/l and initial concentration of Co 89.36 mg/l, which lead to the maximum model-predicted removal percentage as 52.77% removal for Co and 47.33% removal for Ni. The batch adsorption experiment was re-performed at the obtained optimum settings. In this case, the experimentally-measured removal was measured 53.99% for Co and 46.01% for Ni. The outcome verified the rationality of the optimization and the advanced model.

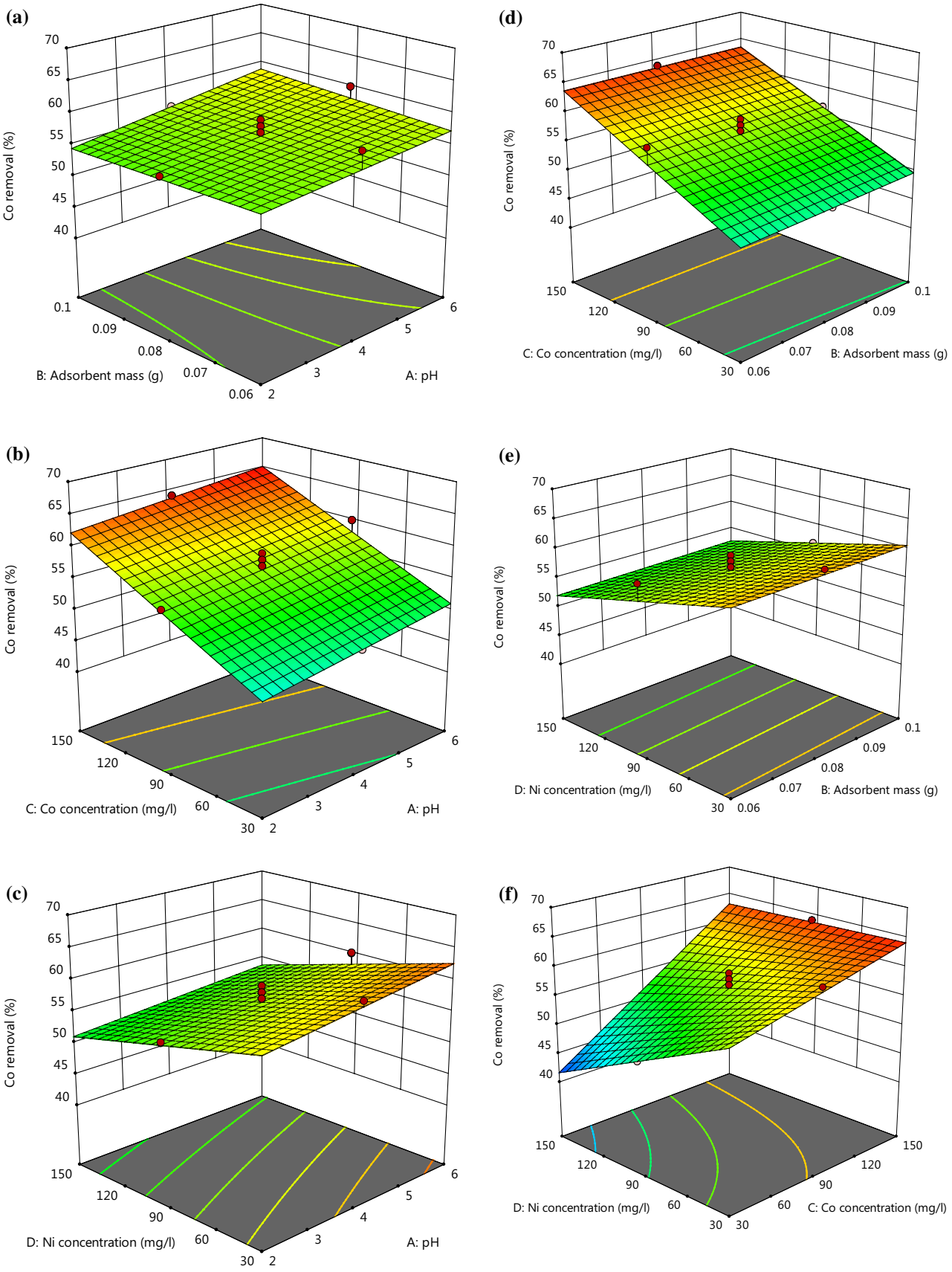
(a)
Co removal (%)
70
65
60
55
50
45
40
0.1
0.09
0.08
0.07
0.06
B: Adsorbent mass (g)
2
3
4
5
6
A: pH
(d)
Co removal (%)
150
120
90
60
30
C: Co concentration (mg/l)
0.06
0.07
0.08
0.09
0.1
B: Adsorbent mass (g)
(b)
Co removal (%)
C: Co concentration (mg/l)
A: pH
(e)
Co removal (%)
D: Ni concentration (mg/l)
B: Adsorbent mass (g)
(c)
Co removal (%)
D: Ni concentration (mg/l)
A: pH
(f)
Co removal (%)
D: Ni concentration (mg/l)
C: Co concentration (mg/l)

◂**Fig. 5** 3D plots of the binary interactions of the variables: Interaction among pH, adsorbent mass (the gram of *C. indica*), and initial concentration on the Co removal

Contact time experiments for Ni and Co adsorption

The impact of contact time on the adsorption of Ni and Co by *C. indica* is shown in Fig. 7. Optimal condition: pH of 5.9, adsorbent mass of 0.06 g, initial concentration of Ni 91.94 and initial concentration of Co 89.36 were used to conduct contact time experiments at 25 °C. Contact time changes from 10 to 180 min. Figure 7 shows that 90% of Ni and Co were adsorbed by *C. indica* in the first 70 min. This is because of the empty active sites on the surface of *C. indica* at the beginning of the adsorption process. Also, a high concentration of Ni and Co can raise the adsorption capacity of *C. indica* at the starting points of the adsorption process. At the end of the adsorption process, reducing the number of active sites causes the reduction of Ni and Co adsorption rate. Therefore, the contact time of 180 min was selected to perform equilibrium experiments. Similarly, 180 min contact time was authenticated by the previously published studies for Ni and Co biosorption using brown algae (Liu et al. 2009; Abdulrazzaq et al. 2014).

Isotherm study for Ni and Co adsorption

Table 6 shows the extended Langmuir and extended Freundlich isotherm parameters at the optimized conditions, including a pH of 5.9, the adsorbent mass of 0.06 g, initial concentration of Ni 91.94 mg/l and initial concentration of Co 89.36 mg/l. The isotherm parameters were conducted at a contact time of 180 min and a temperature of 25 °C. The more value of R^2 signifies the better isotherm model for the adsorption of Ni and Co using *C. indica*. The parameter values of isotherms models for single-metal-component systems and binary-metal-component systems have been shown in Tables 2 and 6, respectively. The equilibrium data for *C. indica* better obeyed the extended Freundlich isotherm for both Co and Ni. Table 6 shows that the extended Langmuir isotherm calculates the maximum adsorption capacity of 67.09 and 71.13 for Ni(II) and Co(II), respectively. Therefore, the biosorption process occurs on heterogeneous surfaces and the concentration of adsorbed Co and Ni ions can affect adsorption capacity.

Alginate plays a pivotal role to adsorb heavy metal ions in the brown algae (Kumar et al. 2018). Figure 8 shows the molecular structure of alginate. The more selectively adsorption of Co by *C. indica* than Ni can be attributed to the direction, form and the gap between indents of glucuronic acid (G), which form a more appropriate complex with Co than mannuronic acid (M), that lead to allow Co ions to enter the structure (Hamedy et al. 2000).

Based on the experimental data, curve-fitting for the extended Freundlich and extended Langmuir isotherms has been shown in Fig. 9. For both Co and Ni, the positive correlations between experimental data (q exp) and calculated-adsorption (q cal) were demonstrated by the extended Freundlich isotherm. The regression correlation coefficient (R^2) values of extended Langmuir isotherm were 0.97 and 0.94 for Ni and Co, respectively, which are less than the values of the regression correlation coefficient (0.98) values of extended Freundlich isotherm for both Co (II) and Ni (II). Consequently, extended Freundlich is the best model for Co (II) and Ni (II) adsorption.

Adsorption process kinetics

The regression correlation coefficient value (R^2) was 0.97 for both Ni and Co when using the intra-particle diffusion model, which is more than the calculated R^2 of the pseudo-first-order and pseudo-second-order models for Ni and Co biosorption using *C. indica*. Therefore, the intra-particle diffusion model was obeyed more closely by the experimental data for both Ni and Co biosorption using *C. indica*. Table 7 shows that the intra-particle diffusion model determines the maximum adsorption capacity of 69.78 and 75.55 for Ni (II) and Co (II), respectively. Based on the principles of the intra-particle diffusion model, the biosorption process was distributed to three stages, including the rapid adsorption, the gradual inner diffusion step and the ending equilibrium step (Hubbe et al. 2019).

Conclusion

The initial concentrations of Ni and Co were the most affecting parameters on the adsorption Co and Ni ions using *C. indica*. Comparisons of Co and Ni biosorption capacity of treated brown algae, *Cystoseria indica*, indicate that the

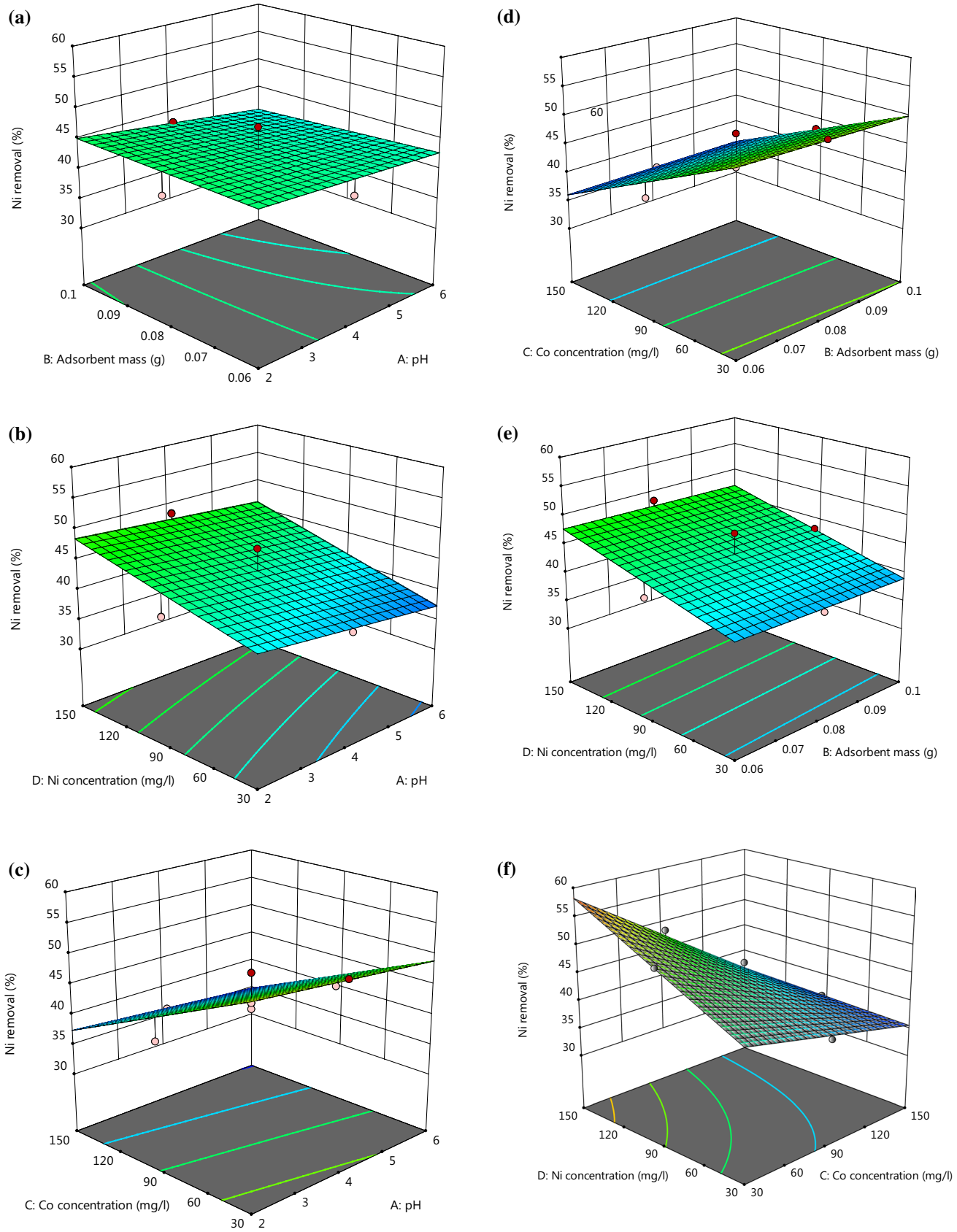

Fig. 6 3D plots of the binary interactions of the variables: Interaction among pH, adsorbent mass (the gram of *C. indica*), and initial concentration on the Ni removal

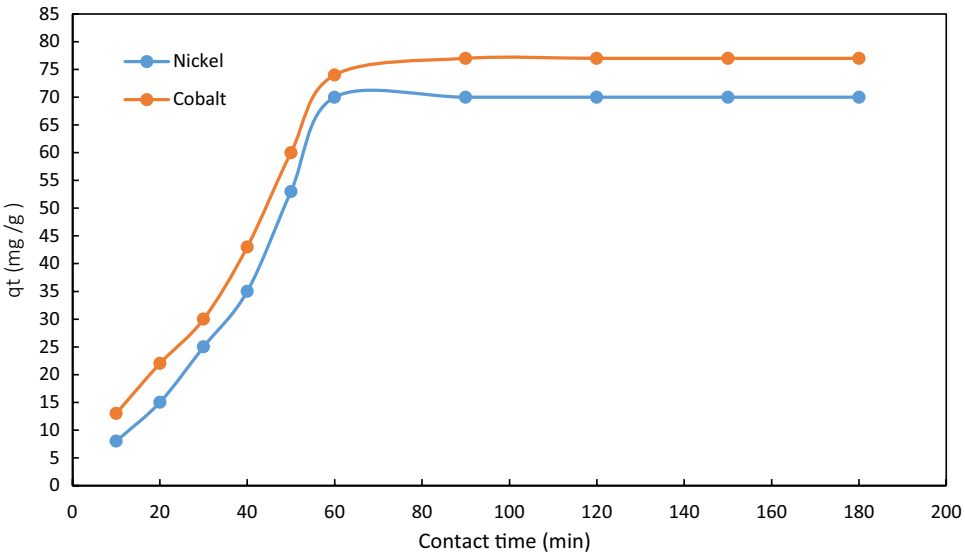

Fig. 7 Contact time experiments for biosorption of Ni(II) and Co(II) using *C. indica*

Table 6 Isotherm parameters for the simultaneous adsorption of Ni and Co by NaCl– pretreated *C. indica* at optimized conditions

Isotherms	Parameters	Ni	Co
Extended Langmuir	q_m (mg/g)	69.99	75.21
	K_L (L/mg)	0.19	0.28
	R^2	0.97	0.94
Extended Freundlich	x	0.006	0.05
	y	1.10	3.11
	z	0.05	0.20
	R^2	0.98	0.98

maximum sorption capacity for Co at an optimum pH of 5.9 was 75.21 mg/L, whereas the maximum Ni biosorption capacity at an optimum pH of 5.9 was 69.99 mg/L. The optimum conditions of the biosorption process were discovered, pH of 5.9, the adsorbent mass of 0.06 g, initial concentration of Ni 91.94 mg/l and initial concentration of Co 89.36 mg/l. The simultaneous biosorption of Ni and Co obeyed the extended Freundlich isotherm. The kinetic behavior of the equilibrium data for Ni and Co sorption by *C. indica* is best explained by the intra-particle diffusion kinetic model.

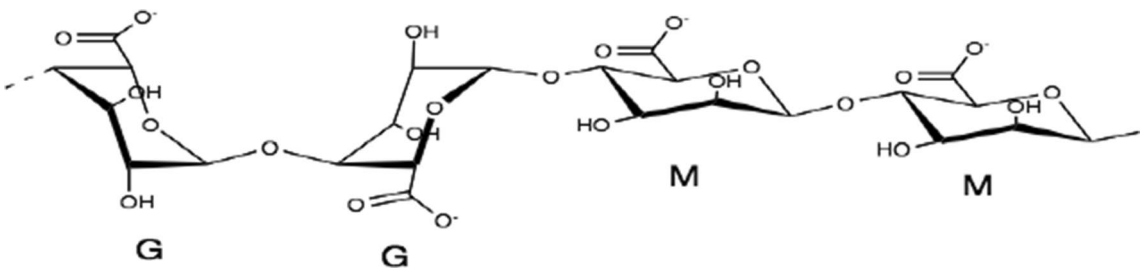

Fig. 8 The molecular structure of alginic acid (Pereira et al. 2017)

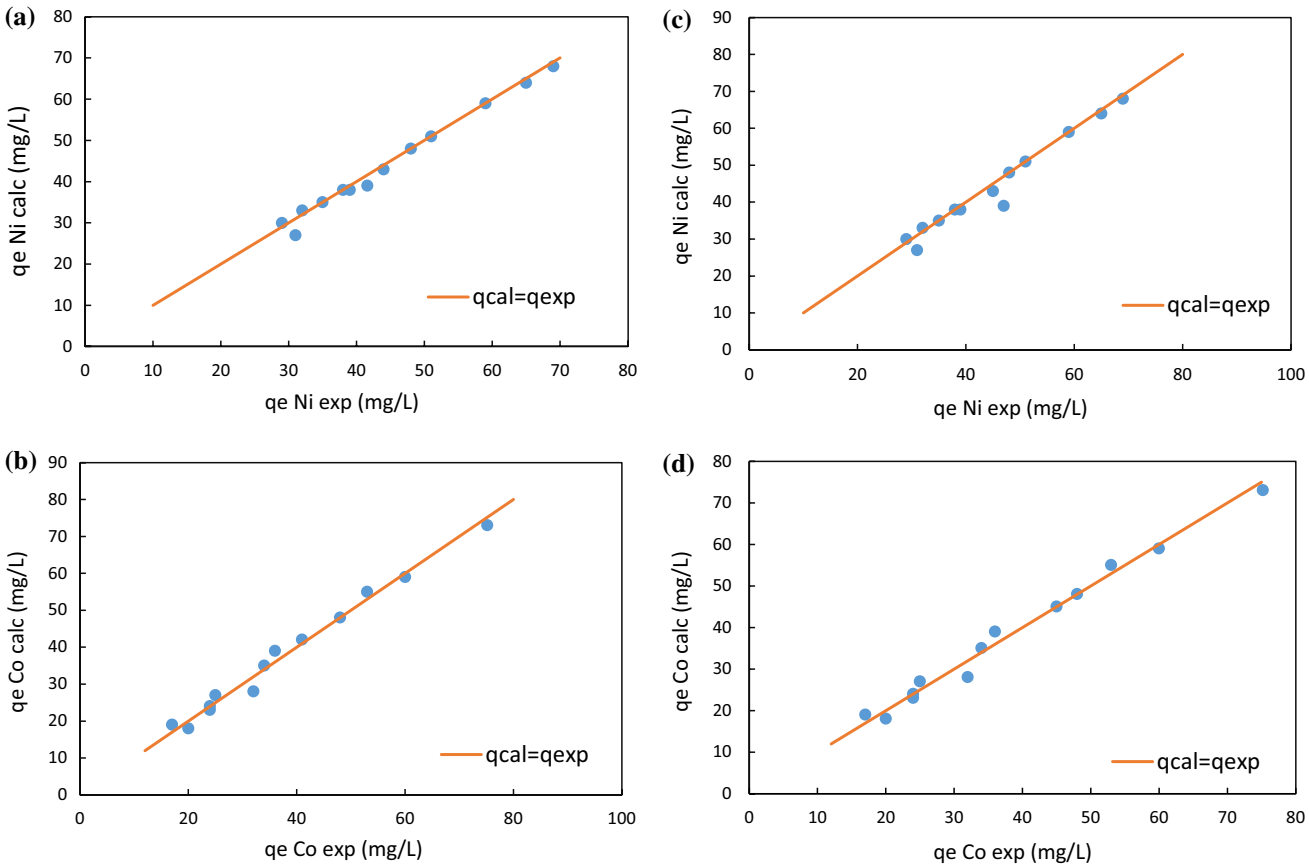

Fig. 9 Comparison of the experimental and calculated equilibrium adsorption values of Co and Ni in binary mixtures

Table 7 Kinetic parameters for the simultaneous adsorption of Ni and Co by NaCl-pretreated C. indica at optimized conditions

Kinetic models	Parameters	Ni	Co
pseudo-first-order	q_e (mg/g)	64.60	71.11
	k_1 (1/min)	0.12	0.27
	R^2	0.89	0.88
pseudo-second-order	q_e (mg/g)	63.75	69.13
	k_2 (g/mg.min)	0.004	0.003
	R^2	0.87	0.86
Intra-particle diffusion	C (mg/g)	69.78	75.55
	k_{id} (mg/g $\text{min}^{0.5}$)	1.99	3.20
	R^2	0.97	0.97

Acknowledgements The authors thankfully acknowledge the support provided by Arak University and Tehran University (2018–2019).

Author contributions MK and PG carried out heavy metal sampling, heavy metal solution analyses, and data organization. AH, MK, and PG participated in interpreting the obtained results and organizing the manuscript. All authors read and approved the final manuscript.

Funding Not applicable.

Compliance with ethical standards

Conflict of interests The authors declare that they have no competing interests.

Availability of data and materials Not applicable.

References

A-Davisa T, Volesky B, Mucci A (2003) A review of the biochemistry of heavy metal bio sorption by brown algae. J Water Res 37:4311–4330

Abdulrazzaq H, Jol H, Husni H, Abu-Bakr R (2014) Characterization and stabilisation of biochars obtained from empty fruit bunch, wood, and rice husk. J BioResources 9:2888–2898

Akbari M, Hallajisani A, Keshtkar A-R, Shahbeig H, Ghorbanian S-A (2015) Equilibrium and kinetic study and modeling of Cu(II) and Co(II) synergistic biosorption from Cu(II)-Co(II) single and binary mixtures on brown algae *C. indica*. J Environ Chem Eng 3:140–149

Askari M, Salehi E, Ebrahimi M, Barati A (2019) Application of breakthrough curve analysis and response surface methodology

for optimization of a hybrid separation system consisting of fixed-bed column adsorption and dead-end depth filtration. J Chem Eng Process Process Intensif 143:107594
Bilal M, Shah JA, Ashfaq T, Gardazi SMH, Tahir AA, Pervez A, Haroon H, Mahmood Q (2013) Waste biomass adsorbents for copper removal from industrial wastewater—a review. J Hazard Mater 263:322–333
Chen Z, Ma W, Han M (2008) Biosorption of Ni and copper and to treated algae (Undriapinnatifida); Application of isotherm and kinetics study. J Hazard Mater 155:327–333
Daraei P, Madaeni SS, Salehi E, Ghaemi N, Sadeghi Ghari H, Khadivi MA, Rostami E (2013) Novel thin film composite membrane fabricated by mixed matrix nanoclay/chitosan on PVDF microfiltration support: preparation, characterization and performance in dye removal. J Membr Sci 436:97–108
De France F-P, Tavares A-P-M, Da Costa A-C-A (2002) Calcium interference with continuous bio sorption of Zinc by sargassum SP. (Phaeophyta) in tubular laboratory reactors. J Bioresour Technol 83:159–163
Esmaeili A, Aghababai Beni A (2015) Biosorption of Ni and Co from plant effluent by Sargassum glaucescens nanoparticles at new membrane reactor. Int J Environ Sci Technol 12:2055
Fan Huan H-J, Tsai Y-S, Furuya E (2008) Prediction of individual Freundlich isotherms from binary and ternary phenolic compounds mixtures. J Chemosphere 71:886–893
Pereira RF, Sousa A, Barrias CC, Bayat A, Granja PL, Bártolo PJ (2017) Advances in bioprinted cell-laden hydrogels for skin tissue engineering. J Biomanuf Rev 2:1
Ferraz AI, Amorim C, Tavares T, Teixeira JA (2015) Chromium (III) biosorption onto spent grains residual from brewing industry: equilibrium, kinetics and column studies. Int J Environ Sci Technol 12(2):1591–1602
Gaikwad M-S, Balomajumder C (2017) Simultaneous electrosorptive removal of chromium(VI) and fluoride ions by capacitive deionization (CDI): multicomponent isotherm modeling and kinetic study. J Separ Purif Technol 182:272–281
Gupta A, Balomajumder Ch (2015) Simultaneous removal of Cr(VI) and phenol from binary solution using Bacillus sp. immobilized onto tea waste biomass. J Water Process Eng 6:1–10
Hashim MA, Mukhopadhyay S, Sahu JN, Sengupta B (2011) Remediation technologies for heavy metal contaminated groundwater. J Environ Manage 92:2355–2388
Hosseini SS, Bringas E, Tan NR, Ortiz I, Ghahramani M, Alaei Shahmirzadi MA (2016) Recent progress in development of high performance polymeric membranes and materials for metal plating wastewater treatment: a review. J Water Process Eng 9:78–110
Hadi P, Barford J, McKay G-M (2013) Synergistic effect in the simultaneous removal of binary Co–Ni heavy metals from effluents by a novel e-waste- derived material. J Chem Eng 228:140–146
Hamdy A (2000) Biosorption of heavy metals by marine algae. J Current Microbiol 4:232
Hubbe MA, Azizian S, Douven S (2019) Implications of apparent pseduo-second-order adsorption kinetics onto cellulosic materials: a review. J Bioresour 14(3):7582–7626
John Babu D, King P, Prasanna Kumar Y (2019) Optimization of Cu (II) biosorption onto sea urchin test using response surface methodology and artificial neural networks. Int J Environ Sci Technol 16:1885
Khajavian M, Wood D, Hallajsani A, Majidian N (2019) Simultaneous biosorption of nickel and cadmium by the brown algae Cystoseria indica characterized by isotherm and kinetic models. Appl Biol Chem 62:69
Khosravi R, Azizi A, Ghaedrahmati R, Gupta VK, Agarwal S (2017) Adsorption of gold from cyanide leaching solution onto activated carbon originating from coconut shell—optimization, kinetics and equilibrium studies. J Ind Eng Chem 54:464–471
Kim S-U, Owens V-N, Kim S-Y, Hong C-O (2017) Effect of different way of bottom ash and compost application on phytoextractability of cadmium in contaminated arable soil. Appl Biol Chem 60(4):353–362
Kumar M, Singh A-K, Sikandar M (2018) Study of sorption and desorption of Cd(II) from aqueous solution using isolated green algae Chlorella vulgaris. J Appl Water Sci 8:225
Leng L, Yuan X, Huang H, Shao J, Wang H, Chen X, Zeng G (2015) Bio-char derived from sewage sludge by liquefaction: characterization and application for dye adsorption. J Appl Surf Sci 346:223–231
Liang Y, Chen JQ, Mei J, Chang JJ, Wang QY, Wan GS, Yin BY (2019) Characterization of Cu and Cd biosorption by Pseudomonas sp. strain DC-B3 isolated from metal mine soil. Int J Environ Sci Technol 16:4035
Li J, Chen J, Chen S (2018) Supercritical water treatment of heavy metal and arsenic metalloid-bioaccumulating-biomass. J Ecotoxicol Environ Saf 157:102–110
Liu Y, Cao Q, Luo F, Chen J (2009) Biosorption of $Cd2^+$, $Cu2^+$, $Ni2^+$ and $Zn2^+$ ions from aqueous solutions by pretreated biomass of brown algae. J Hazard Mater 163:931–938. https://doi.org/10.1016/j.jhazmat.07.046.18755544
Luo Z, Wang Z, Yan Y, Li J, Yan C, Xing B (2018) Titanium dioxide nanoparticles enhance inorganic arsenic bioavailability and methylation in two freshwater algae species. J Environ Pollut 238(5):631–637
Montazer-Rahmatia MM, Rabbania P, Abdolalia A, Keshtkarb AR (2011) Kinetics and equilibrium studies on biosorption of cadmium, lead, and Ni ions from aqueous solutions by intact and chemically modified brown algae. J Hazard Mater 185(1):401–407
Mudhoo A, Garg V-K, Wang SS (2012) Heavy metals: toxicity and removal by biosorption. In: Lichtfouse E, Schwarzbauer J, Robert D (eds) Environmental chemistry for a sustainable world. Springer, Berlin, pp 379–442
Naseem K, Begum R, Wu W, Usman M, Irfan A, Al-Sehemi A, Farooqi Z-H (2018) Adsorptive removal of heavy metal ions using polystyrene-poly(N-isopropylmethacrylamide-acrylic acid) core/shell gel particles: Adsorption isotherms and kinetic study. J Mol Liquids 277:522–531
Nas SM, Calimli HM, Burhan H, Yilmaz M, Mustafo DS (2019) Sen F (2019) Synthesis, characterization, kinetics and adsorption properties of Pt-Co@GO nano-adsorbent for methylene blue removal in the aquatic mediums using ultrasonic process systems. J Mol Liq 296:112100
Negm NA, Abd El Wahed MG, Hassan ARA, Abou Kana MTH (2018) Feasibility of metal adsorption using brown algae and fungi: Effect of biosorbents structure on adsorption isotherm and kinetics. J Molliq 264(15):292–305
Nuhoglu Y, Malkoc E, Gurses A, Canpolat N (2002) The removal of cu (II) from aqueous solutions by Ulothrix Zonata. J Bioresour Technol 85:331–333
Ojedokun AT, Bello OS (2016) Sequestering heavy metals from wastewater using cow dung. Water Resour Ind 13:7–13
Ozdemir S, Kilinc E, Fatih S (2020) A novel biosorbent for preconcentrations of Co(II) and Hg(II) in real samples. Sci Rep 10:455
Park J-H, Ok Y-S, Kim S-H, Kang S-W, Cho J-S, Heo J-S, Delaune R-D, Seo D-C (2015) Characteristics of biochars derived from fruit tree pruning wastes and their effects on lead adsorption. J Korean Soc Appl Biol Chem 58(5):751–760
Pinnola A, Formighieri C, Bassi R (2019) Algae: a new biomass resource. In: Kaltschmitt M (ed) Energy from organic materials (Biomass). Encyclopedia of Sustainability Science and Technology Series. Springer, New York, NY, pp 165–197
Putro J-N, Santoso S-P, Ismadji S, Ju Y-H (2017) Investigation of heavy metal adsorption in binary system by nanocrystalline cellulose e

Bentonite nanocomposite: Improvement on extended Langmuir isotherm model. J Microporous Mesoporous Mater 246:166–177
Rasool K, Lee DS (2015) Characteristics, kinetics and thermodynamics of Congo Red biosorption by activated sulfidogenic sludge from an aqueous solution. Int J Environ Sci Technol 12:571
Şahan T (2019) Application of RSM for Pb(II) and Cu(II) adsorption by bentonite enriched with eSH groups and a binary system study. J Water Process Eng 31:100867
Salehi E, Gavari N, Chehrei A, Amani S, Amani N, Zaghi K (2019) Efficient separation of triglyceride from blood serum using Cinnamon as a novel biosorbent: adsorption thermodynamics, kinetics, isothermal and process optimization using response surface methodology. J Process Biochem 77:122–136
Salehi E, Madaeni SS (2014) Influence of poly(ethylene glycol) as pore-generator on morphologyand performance of chitosan/poly(vinyl alcohol) membrane adsorbents. J Appl Surf Sci 288:537–541
Sari A, Tuzen M (2008) Biosorption of Cadmium (II) from aqueous Solution by red argue (ceramiumvirgatum): equilibrium, Kinetic and thermodynamic studies. J Haz Mat 157(2–3):448–454
Senthilkumar R, Vijayaraghavan K, Thilakavathi M, Iyer PVR, Velan M (2006) Seaweeds for the remediation of wastewaters contaminated with zinc (II) ions. J Hazardous Mater 136(3):791–799
Sinaeia M, Loghmani M, Bolouki M (2018) Application of biomarkers in brown algae (*Cystoseria indica*) to assess heavy metals (Cd, Cu, Zn, Pb, Hg, Ni, Cr) pollution in the northern coasts of the Gulf of Oman. Ecotoxicol Environ Saf 164:675–680
Taghiganji M, Khosravi M, Rakhshaee R (2005) R. Int J Environ Sci Technol 1(4):265–271
Villar da Gama B-M, Nascimento G-E, Cesar D, Sales S, Rodríguez-Díaz J-M, de Menezes B, Barbosa C-M-B, Duarte M-M-M-B (2018) Mono and binary component adsorption of phenol and cadmium using adsorbent derived from peanut shells. J Cleaner Prod 201:219–228
Volesky B (2001) Detoxification of metal-bearing effluents: biosorption for the next century. J Hydrometall 59:203–216
Volesky B, Naja G-M (2011) Biosorption for industrial application biosorption process fundamentals and a pilot design. Biosorption Ind Appl 6:25
Xiao B, Dai Q, Yu X, Yu P, Zhai S, Liu R, Guo X, Liu J, Chen H (2018) Effects of sludge thermal-alkaline pretreatment on cationic red X-GRL adsorption onto pyrolysis biochar of sewage sludge. J Hazard Mater 343:347–355
Xiong Y, Xu J, Shan W, Lou Z, Fang D, Zang S, Han G (2013) A new approach for rhenium(VII) recovery by using modified brown-algae Laminaria japonica adsorbent. J Bioresource Technol 127:464–472
Xu L, Shen J, Marinova D, Guo X, Sun F, Zhu F (2013) Changes of public environmental awareness in response to the Taihu blue-green algae bloom incident in China. J Environ Develop Sustain 15(5):1281–1302
Yalçın S, Sezer S, Apak R (2012) Characterization and lead(II), cadmium(II), Ni(II) biosorption of dried marine brown macro algae Cystoseira barbata. Environ Sci Pollut Res 19(18):3118–3125